

Advanced Predictive Structural Health Monitoring in High-Rise Buildings Using Recurrent Neural Networks

Ghaffari, Abbas; Shahbazi, Yaser ; Mokhtari Kashavar, Mohsen; Fotouhi, Mohammad; Pedrammehr, Siamak

DOI

[10.3390/buildings14103261](https://doi.org/10.3390/buildings14103261)

Publication date

2024

Document Version

Final published version

Published in

Buildings

Citation (APA)

Ghaffari, A., Shahbazi, Y., Mokhtari Kashavar, M., Fotouhi, M., & Pedrammehr, S. (2024). Advanced Predictive Structural Health Monitoring in High-Rise Buildings Using Recurrent Neural Networks. *Buildings*, 14(10), Article 3261. <https://doi.org/10.3390/buildings14103261>

Important note

To cite this publication, please use the final published version (if applicable). Please check the document version above.

Copyright

Other than for strictly personal use, it is not permitted to download, forward or distribute the text or part of it, without the consent of the author(s) and/or copyright holder(s), unless the work is under an open content license such as Creative Commons.

Takedown policy

Please contact us and provide details if you believe this document breaches copyrights. We will remove access to the work immediately and investigate your claim.

Article

Advanced Predictive Structural Health Monitoring in High-Rise Buildings Using Recurrent Neural Networks

Abbas Ghaffari ¹, Yaser Shahbazi ¹, Mohsen Mokhtari Kashavar ¹ , Mohammad Fotouhi ^{2,*} and Siamak Pedrammehr ^{3,*} 

¹ Faculty of Architecture and Urbanism, Tabriz Islamic Art University, Tabriz 5164736931, Iran; ghaffari@tabriziau.ac.ir (A.G.); y.shahbazi@tabriziau.ac.ir (Y.S.); mo.mokhtari@tabriziau.ac.ir (M.M.K.)

² Faculty of Civil Engineering and Geosciences, Delft University of Technology, 2628 CN Delft, The Netherlands

³ Faculty of Design, Tabriz Islamic Art University, Tabriz 5164736931, Iran

* Correspondence: m.fotouhi-1@tudelft.nl (M.F.); s.pedrammehr@tabriziau.ac.ir (S.P.)

Abstract: This study proposes a machine learning (ML) model to predict the displacement response of high-rise structures under various vertical and lateral loading conditions. The study combined finite element analysis (FEA), parametric modeling, and a multi-objective genetic algorithm to create a robust and diverse dataset of loading scenarios for developing a predictive ML model. The ML model was trained using a recurrent neural network (RNN) with Long Short-Term Memory (LSTM) layers. The developed model demonstrated high accuracy in predicting time series of vertical, lateral (X), and lateral (Y) displacements. The training and testing results showed Mean Squared Errors (MSE) of 0.1796 and 0.0033, respectively, with R^2 values of 0.8416 and 0.9939. The model's predictions differed by only 0.93% from the actual vertical displacement values and by 4.55% and 7.35% for lateral displacements in the Y and X directions, respectively. The results demonstrate the model's high accuracy and generalization ability, making it a valuable tool for structural health monitoring (SHM) in high-rise buildings. This research highlights the potential of ML to provide real-time displacement predictions under various load conditions, offering practical applications for ensuring the structural integrity and safety of high-rise buildings, particularly in high-risk seismic areas.



Citation: Ghaffari, A.; Shahbazi, Y.; Mokhtari Kashavar, M.; Fotouhi, M.; Pedrammehr, S. Advanced Predictive Structural Health Monitoring in High-Rise Buildings Using Recurrent Neural Networks. *Buildings* **2024**, *14*, 3261. <https://doi.org/10.3390/buildings14103261>

Academic Editor: Chunwei Zhang

Received: 5 September 2024

Revised: 12 October 2024

Accepted: 13 October 2024

Published: 15 October 2024



Copyright: © 2024 by the authors. Licensee MDPI, Basel, Switzerland. This article is an open access article distributed under the terms and conditions of the Creative Commons Attribution (CC BY) license (<https://creativecommons.org/licenses/by/4.0/>).

Keywords: SHM; RNN; LSTM; FEA; optimization; high-rise structure

1. Introduction

Structural health monitoring is a critical aspect of structural engineering that involves the continuous or periodic monitoring and assessment of structures to detect damage and ensure their safety, reliability, and longevity. This process integrates various sensing technologies, data analysis techniques, and computational models to identify potential issues such as material fatigue, cracking, and deformation, ultimately helping to avoid catastrophic failures in infrastructure [1,2]. SHM systems are widely applied in the monitoring of bridges, buildings, and other civil structures. These systems utilize smart sensors, such as piezoelectric, optical fiber, and magnetostrictive sensors, to capture real-time data on structural performance. These data are then analyzed using advanced techniques like ML and artificial intelligence to identify anomalies, enabling the early detection of structural issues [2,3].

Since the construction of high-rise buildings began, research on their various aspects has become a key focus [4]. Gunel and Ilgin [5] reviewed the evolution of tall building structures, noting a shift from gravity to lateral loads like wind and earthquakes. As cities and architecture have advanced, buildings have become taller and more complex, posing new challenges for maintenance, safety, and structural integrity. SHM plays a crucial role in addressing these challenges, focusing on damage detection and overall building health through population-based models and dynamic monitoring during construction. Astorga et al. [6] highlight SHM techniques using transfer learning and Gaussian mixture

models to classify damage and aid decision-making. Nicoletti et al. [7] stress dynamic monitoring during construction to track modal property changes and prevent errors. Xu et al. [8] studied the dynamic characteristics of a 600-meter skyscraper with an ATMD during Super Typhoon Saola, while Zhou et al. [3] analyzed the time-varying dynamics of a 420 m building during typhoons. Zhou et al. [9] used social sensing and computer vision to monitor the Xiamen twin towers during Super Typhoon Soksuri. Li et al. [10] assessed Typhoon Vicente's impact on a 420 m building in Hong Kong, comparing wind tunnel predictions with field data. Comprehensive reviews for vibration-based signal processing techniques for structural health monitoring (SHM) have also been presented [11,12]. The reviews categorized methods into time- and frequency-domain approaches for dynamic feature extraction and structural damage detection, addressing the strengths and limitations of each technique. Mousavi et al. [13] investigated a new method combining empirical wavelet transform (EWT) and artificial neural networks (ANN) for damage detection in a steel truss bridge. The approach efficiently detects and classifies damage using signal features like energy, RMS, and entropy.

Wireless sensor networks (WSNs) are essential in advancing SHM for high-rise buildings, where ML algorithms process sensor data to detect anomalies and predict failures [14]. These networks enable real-time, continuous monitoring of critical parameters like strain, temperature, and displacement, providing valuable insights into building health.

Finite element analysis (FEA) is a powerful computational method in structural monitoring, assessing how a structure behaves under various loading conditions. It predicts a structure's reaction to load and environmental factors [15]. FEA is often combined with sensor data to validate and improve the accuracy of ML models in SHM. This hybrid approach enhances the predictive capabilities of monitoring systems by training ML models with FEA simulation results [16]. Ruggieri et al. [17] used FEA to simulate a building's response to vibrations during dredging at Bari Port, ensuring structural safety.

SHM has evolved to provide continuous condition monitoring and real-time analysis, supporting predictive maintenance and enhancing the durability of high-rise buildings by integrating ML. Recent SHM advancements use ML algorithms to process large sensor datasets and detect patterns and anomalies. High-rise buildings are vulnerable to environmental forces like wind and earthquakes. ML is now vital for automating damage detection, as traditional methods like Fourier transforms and wavelet analysis were limited by noise and environmental variability. Early ML applications in SHM, such as ANN [18], SVM [19] and genetic algorithms [20], focused on feature classification but faced challenges in real-world conditions. Lin et al. [21] demonstrated that ML algorithms provide more accurate predictions of crosswind load effects on tall buildings. Shahbazi et al. [22] showed that ANNs work well with small datasets, producing solid, generalizable results. Optimization and ANN-based algorithms have been used for damage detection in complex geometries [23,24]. For instance, Zhou et al. [25] developed an LSTM model to estimate the displacement of a 420 m building during Super Typhoon Mangkhut, validated by field measurements. Parisi et al. [26] developed an ML method using a convolutional neural network (CNN) to detect damage in steel truss bridges, achieving 93% accuracy in classifying raw strain measurement data. Cabboi et al. [27] applied a damage assessment strategy to historic towers, integrating vibration monitoring with FE model updates to improve damage localization accuracy. Ierimonti et al. [28] introduced a Bayesian model for tracking structural degradation over time, which was validated in a school building. García-Macías, and Ubertini advanced SHM automation with statistical methods and real-time monitoring models [29]. Sapidis et al. [30] introduced a 1-D CNN for autonomously detecting cracks in fiber-reinforced concrete, utilizing piezoelectric transducers to capture electromechanical impedance data and achieving 95.24% accuracy. Similarly, Ali and Cha [31] developed a deep learning-based approach for subsurface damage detection in steel bridges, utilizing infrared thermography and a modified deep inception neural network (DINN). Their method achieved 96% accuracy and 97.79% specificity, validated through ultrasonic pulse velocity tests. Sen et al. [32] proposed a multi-component deconvolution interferometry

technique for predicting seismic structural responses, addressing sparse sensor issues. Their surrogate model, tested on Groningen structures, demonstrated high accuracy despite measurement uncertainties. Yang et al. [33] employed infrared thermal imaging and an enhanced Faster R-CNN to detect cracks in steel, achieving 95.54% accuracy and 92.41% mean average precision, surpassing conventional methods. In the realm of smart buildings, Yu et al. [34] developed a deep convolutional neural network (DCNN) that processes raw vibration data for automatic damage detection without requiring manual feature selection and demonstrated high accuracy in tests on a five-story building under seismic loads.

Although there are many studies in SHM, research specifically focused on SHM for high-rise structures is relatively limited, with most studies focusing on numerical methods and sensor-based approaches. These structures' critical importance necessitates exploring more accurate and practical forecasting methods. Therefore, the main goal of this study is to develop a predictive ML model to evaluate the conditions of high-rise buildings after imposing various and previously unseen loads in both vertical (across various floors) and lateral directions. This framework effectively examines building responses regarding vertical and lateral displacements. Alongside this critical challenge, and despite the advances ML has brought to SHM, several challenges remain in developing ML for SHM. The first and foremost requirement for high-performance ML models is extensive, high-quality datasets for training. ML models can be sensitive to the quality of input data, which can be challenging to obtain, particularly in the case of rare events such as extreme weather or seismic activity [15,35]. Another challenge is the interpretability of ML models, as many state-of-the-art techniques, especially deep learning models, operate as "black boxes" with limited transparency in how predictions are made [36,37]. This research addressed these challenges by numerically analyzing various model configurations using FEA to generate a wide range of high-quality data. Using LSTM layers inside the RNN model, we tried to extend the interpretability of the model.

Following the introduction, the methodology for developing the FEA and ML models is discussed. The results section presents the ML model's performance in predicting the expected targets, and these results are compared with actual values obtained from FEA. Finally, the study concludes with an analysis of the model's effectiveness, addressing its strengths and limitations and providing insights into the implications of these findings for future research and practical applications in high-rise structures SHM. Potential improvements and future directions for enhancing the accuracy and interpretability of ML models in this field are also suggested.

2. Methodology

This research aimed to develop an ML model capable of predicting high-rise building displacement under various vertical and lateral loadings, enabling convenient SHM without requiring extensive FEA simulations. The developed ML model allows users to input different loading scenarios for each floor and façade of the structure, simulating unforeseen situations that might impact the building's integrity. To achieve this objective, we employed a combination of parametric modeling, FEA, optimization techniques, and ML methods. The following sections provide a detailed account of each step in the process.

2.1. Base Structure Modeling

Accurate simulation of various loading conditions requires a precise high-rise building model. For this purpose, we utilized Grasshopper 3D [38], a visual programming language integrated with Rhinoceros 3D, a computer-aided design (CAD) application. Grasshopper 3D provides a flexible and dynamic environment for parametric modeling, enabling easy adjustments to design parameters and rapid iteration of structural configurations. The building model used in this study is a 20-story high-rise structure with a base area of 1200 m², designed with an internal shear core to withstand lateral loads such as wind and earthquakes—a common feature in high-seismic zones such as Tabriz in Iran. Tabriz is classified as a high-risk seismic zone under the Iranian Seismic Code (Standard No. 2800) [39],

with a seismic zone factor (Z) that accounts for the region's expected ground acceleration. The high-rise structure model is presented in Figure 1. The building structure cross sections and material specifications are presented in Table 1.

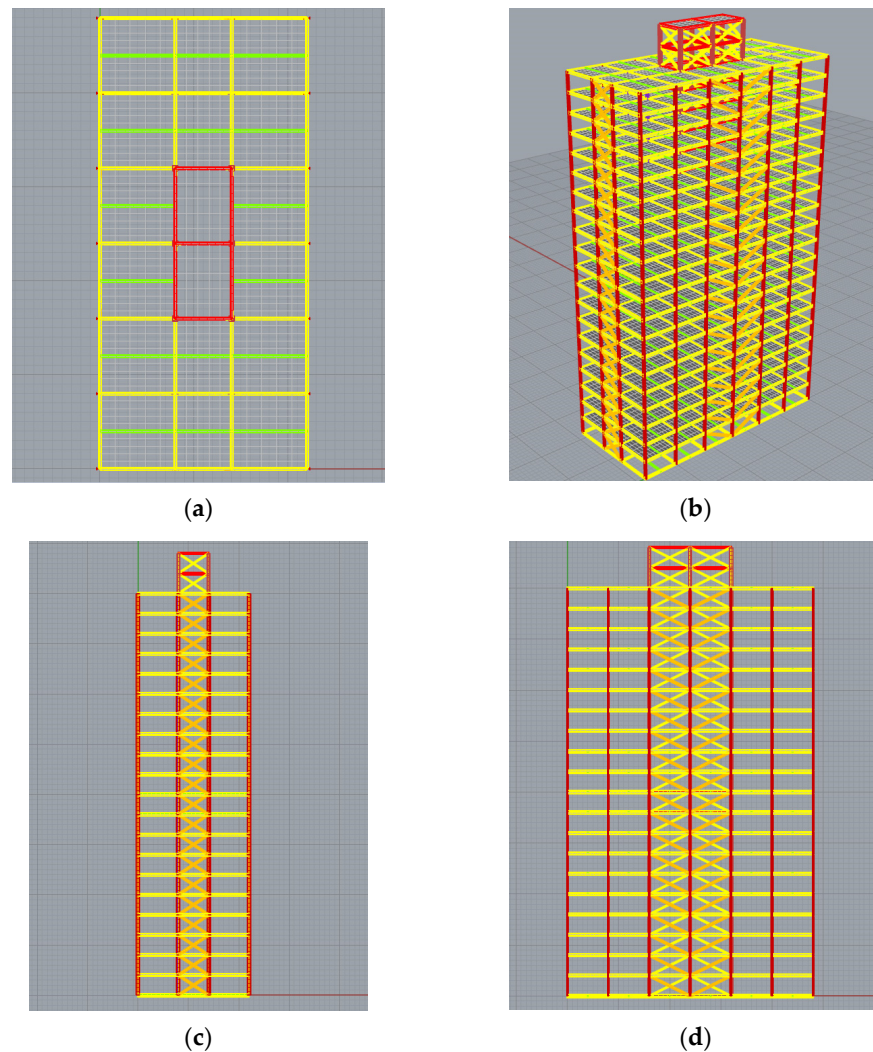


Figure 1. The high-rise structure modeled in Grasshopper and karamba3D: (a) top; (b) perspective; (c) right; and (d) front view.

Table 1. The building structure cross sections and material specifications.

	Dimensions (cm)				Cross Section	Material Properties			
	H	zs	zm	Max Width		Material	E (kN/cm ²)	G12 (kN/cm ²)	G3 (kN/cm ²)
Outer beams	97	48.5	48.5	30	I	Steel	21,000	8076	8076
Inner main beams	87	43.5	43.5	30	I				
Inner sub-beams	62	31	31	30	I				
Exterior columns	80	40	40	80	[]				
Inner columns	80	40	40	80	[]				
Exterior bracing	87	43.5	43.5	30	I				
Shear core beams	52.2	26.1	26.1	30	I				
Shear core columns	60	30	30	60	[]				
Shear core bracing	28.3	14.15	14.15	30	I				
Floor shells	20	-	-	-	-				

2.2. Load Calculations

The seismic analysis was conducted using the Equivalent Lateral Force (ELF) method, a linear static analysis approach. This method simplifies dynamic seismic effects into equivalent static forces distributed across the structure. The seismic base shear was distributed using a triangular distribution, with forces concentrated at the upper stories due to greater displacements. This distribution aligns with typical assumptions in ELF analysis. This approach was suitable given the building's regular geometry and its steel-braced shear core design, which effectively resists lateral loads, including those from wind and earthquakes.

A standard vertical load of 7 kN/m² was applied to each floor. Lateral loads due to seismic activity were calculated following the guidelines of the International Building Code (IBC) [40], as detailed earlier in this paper. Table 2 presents the initial assumption values used in the lateral load calculations.

Table 2. Initial assumptions considered for lateral load calculations.

Building Mass (W)	Seismic Zone Factor (Z)	Importance Factor (I)	Response Modification Factor (R)	Site Coefficient (S)	Spectral Acceleration Coefficient (C(T))	Structure Façade Area (y)
136,524.25 kN	0.35	1.0	6	1.2	1.0 g	3840 m ²

The seismic load (base shear) was distributed across the building's height, with particular attention to the force distribution on the building's façades. The seismic load (base shear) was calculated using the following equations:

Step 1: the empirical formula was used to calculate the building period (T), which was determined to be 1.97 s.

$$T = Ct \times H^{\frac{3}{4}} \quad (1)$$

Step 2: The base shear (V) was calculated using the following equation and determined to be 9556.69 kN:

$$V = \frac{Z \cdot I \cdot W}{R} \times S \times C(T) \quad (2)$$

Step 3: The calculated base shear (V), representing the total lateral force that the building must resist, should be distributed across each square meter of the building's façade to determine the load distribution per square meter of the façade.

$$q = \frac{V}{Face\ Area} \approx 2.49 \text{ kN/m}^2 \quad (3)$$

Step 4: The load should be distributed over the height of the building calculated using the following equation:

$$q_{height} = \frac{q}{H} = 0.0311 \text{ kN/m}^3 \quad (4)$$

Final step: The final load distribution for the lateral (y) load was estimated to be 2.488 kN/m². The lateral (x) load was calculated similarly.

The maximum allowable displacement at the top of a building under earthquake load is typically governed by building codes and standards, which set limits based on the building's height and intended use or occupancy. These limits are usually expressed as a fraction of the building's height. According to ASCE 7-16 [41] Building standards, most structures' maximum allowable drift (displacement) is typically limited to 2% of the building height, particularly for ordinary buildings. For the subject building, this limit equates to a maximum allowable displacement of 1.6 m. For buildings designed to be more rigid, such as those with essential functions (e.g., hospitals and emergency centers), this limit is often further reduced to 1% of the building height.

2.3. Structural Modeling and Analysis

Once the parametric model was developed in Grasshopper and the loads were calculated, we utilized Karamba3D [42], a parametric engineering tool integrated within the Grasshopper environment, to convert the geometric model into a structural model suitable for FEA. Karamba3D facilitates the integration of parameterized geometric models with FEA, enabling quick and accurate structural assessments. The FEA revealed that the maximum displacement under vertical loads was 3.5 cm, while the maximum displacements under lateral loads in the X and Y directions were 6.33 cm and 7.94 cm, respectively. Given the building's 88 m height, these values represent 0.79% and 0.99% of the building height, meeting the ASCE 7-16 standards for maximum allowable drift. The total mass of the building was calculated to be 13,926.64 tons.

2.4. Dataset Generation

We employed a multi-objective genetic algorithm (MOGA) with a parametric model of high-rise buildings to create a robust ML model for predicting structural responses under various conditions. This approach ensured a diverse set of solutions that reflect potential real-world scenarios. Variables such as floor loads and lateral forces from wind and seismic activity were included in the dataset. A total of 7347 distinct solutions were generated, providing a comprehensive dataset for training the ML model. The variables and their respective domains are detailed in Table 3.

Table 3. The variables and their respective domains.

	Min	Max
Lateral load (X direction) (m ² of building façade)	0	6
Lateral load (Y direction) (m ² of building façade)	0	6
Floors 1–20 vertical load (m ²)	0	15

In addition to serving as a dataset generator for the ML model, the framework developed in this research functions as a digital twin of the high-rise building. This digital twin can simulate various loading scenarios to evaluate the building's performance under different conditions. In real-world applications, sensors can monitor actual loads on the structure, enabling continuous SHM and real-time evaluations. Figure 2 presents a flowchart of the developed definitions in Grasshopper and Karamba3D for structural modeling, FEA simulations, and data generation. Figure 3 presents a flowchart of the proposed framework to predict structure displacements in the vertical, lateral X, and lateral Y directions.

2.5. ML Model Development

2.5.1. Data Preprocessing

The first step in developing the ML model involved preparing the dataset for training. The dataset was loaded from a CSV file containing 7347 data points, each representing a distinct combination of load scenarios and corresponding displacements. The input features (X) included the load values applied to each floor (Floor 0 to Floor 20) and lateral forces in both the X and Y directions. The target variables (y) were the vertical and lateral displacements in the X and Y directions.

Given the varying scales of the input features and target variables, it was essential to standardize the data to ensure effective learning by the RNN model. We used StandardScaler from the scikit-learn library to normalize the input features (X) and target variables (y), transforming them to have a mean of 0 and a standard deviation of 1. This scaling process was crucial for stabilizing the training of the RNN model, especially considering the different magnitudes of loads and displacements.

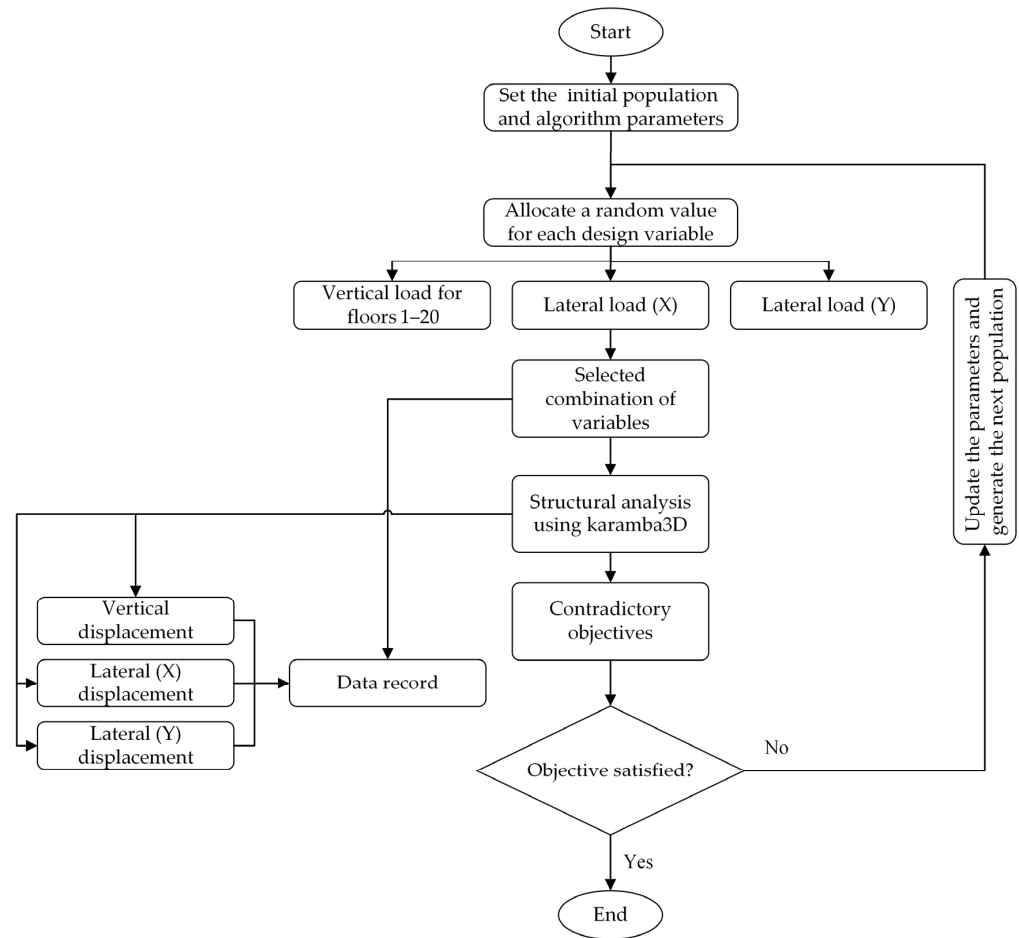


Figure 2. Flowchart of developed definition in grasshopper and karamba3D for data generation.

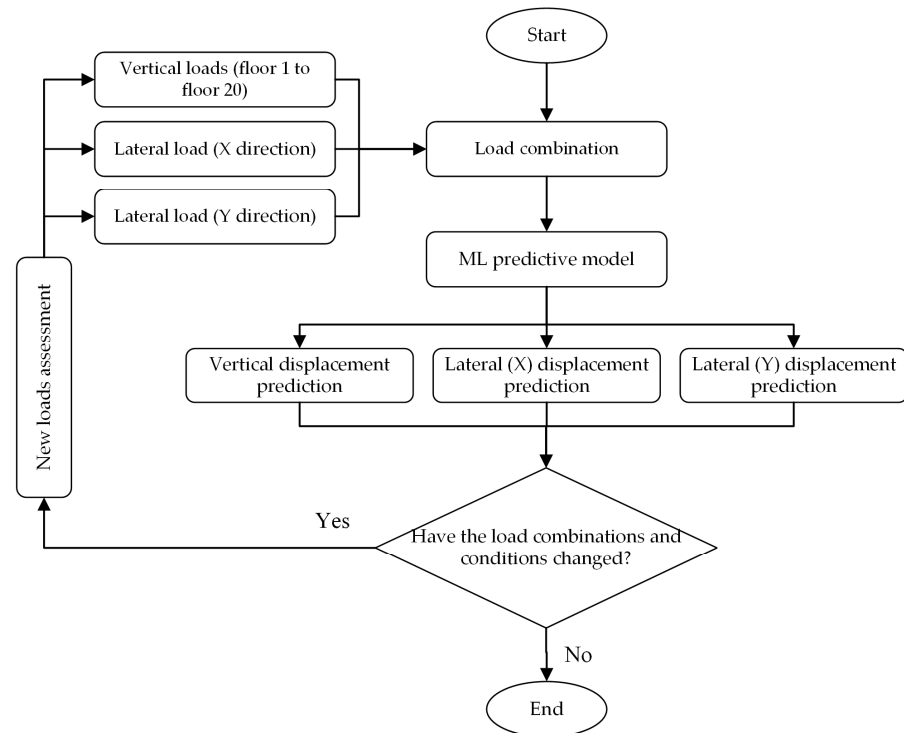


Figure 3. Flowchart of the proposed framework to predict structure displacements.

2.5.2. Model Selection

The choice of an RNN with LSTM layers was based on the need to model sequential dependencies in the data. LSTMs are well suited for time-series and sequence data, making them an optimal choice for predicting displacements under varying loads across multiple floors. Unlike traditional feedforward neural networks, LSTMs maintain a memory of previous states, enabling the model to capture complex temporal relationships between input forces and resulting displacements over time. This architecture was selected to ensure the model could learn patterns that span multiple time steps, which is essential in SHM, where loading conditions are dynamic. Using LSTM layers also reflects a balance between interpretability and performance. More complex architectures, such as Transformer models or DCNN, might provide marginal improvements in accuracy but at the cost of model transparency. In contrast, LSTMs offer a more understandable framework for tracking how predictions change with different load scenarios, which is critical for practical applications in structural engineering. By training the model on a large and varied dataset of 7347 load scenarios, we ensured that the ML model learns patterns that can be traced back to specific conditions. This traceability enhances our understanding of why the ML model makes certain predictions under particular conditions, thereby improving interpretability.

2.5.3. ML Model Architecture

The architecture of the developed model is as follows:

- **Input layer:** The input shape accommodates the scaled features for each floor and lateral load.
- **LSTM layers:** Two LSTM layers were used, with the first layer having 128 units and the second 256 units. The first LSTM layer is set to return sequences, allowing the second LSTM layer to process the output. These LSTM layers capture the temporal dependencies between different load conditions and their resulting displacements.
- **Dropout layers:** To prevent overfitting, dropout regularization was applied after each LSTM layer and before the final dense layer. The dropout rates were set to 30% after the LSTM layers and 50% before the output layer.
- **Dense layer:** To map the learned features to the output space, a fully connected dense layer with 512 neurons and an ReLU activation function was included.
- **Output layer:** The output layer contains three neurons, each corresponding to one of the target displacements: vertical displacement, lateral displacement in the Y direction, and lateral displacement in the X direction.

The model was configured using the Adam optimizer with a learning rate of 0.001.

2.5.4. Performance Metrics and Evaluation

Four key evaluation metrics were used to assess the accuracy and reliability of the developed ML model: Mean Squared Error (MSE), R-squared (R^2), Mean Absolute Error (MAE), and the maximum difference of predicted values from actual values (expressed as a percentage). Each metric was chosen to comprehensively evaluate the model's performance across different aspects of prediction accuracy.

- **Mean Absolute Error (MAE):** This metric represents the average absolute differences between predicted and actual values, offering a straightforward measure of prediction error in the original units. It is particularly valuable for understanding overall model accuracy in regression tasks, especially when all errors are treated equally without overemphasizing large errors [43].
- **Mean Squared Error (MSE):** MSE measures the average of the squares of the errors between predicted and actual values. It provides insight into the magnitude of the prediction error, with lower MSE values indicating better performance. This metric is widely used in regression tasks due to its sensitivity to outliers and large deviations in predictions, making it valuable for detecting significant errors [43].

- R-squared (R^2): The R^2 value, also known as the coefficient of determination, indicates the proportion of the variance in the dependent variable that is predictable from the independent variables. An R^2 value closer to 1 implies a strong correlation and better model fit, while values closer to 0 indicate weaker predictive power [44]. This metric helps quantify how well the model generalizes to unseen data.
- Maximum Difference from Actual Value (%): This residual-based metric expresses the largest deviation between predicted and actual values as a percentage of the actual value. It is particularly useful for understanding the extremes in model performance, which are often critical in structural engineering applications where even small deviations can have significant consequences [45].

3. Results and Discussion

3.1. ML Model Implementation

The developed ML model was trained over 500 epochs with batch sizes of 16 samples, and 20% of the training data were used as a validation set to monitor performance.

Figure 4 displays the Training Loss chart over 500 epochs. Initially, the loss is high (~0.7), but it rapidly decreases and stabilizes around 0.3 after approximately 100–150 epochs. The loss then fluctuates slightly, indicating that the model has learned the training data well, making only minor adjustments in the later epochs. The developed model shows significant progress early on, with minimal further improvements as training continues.

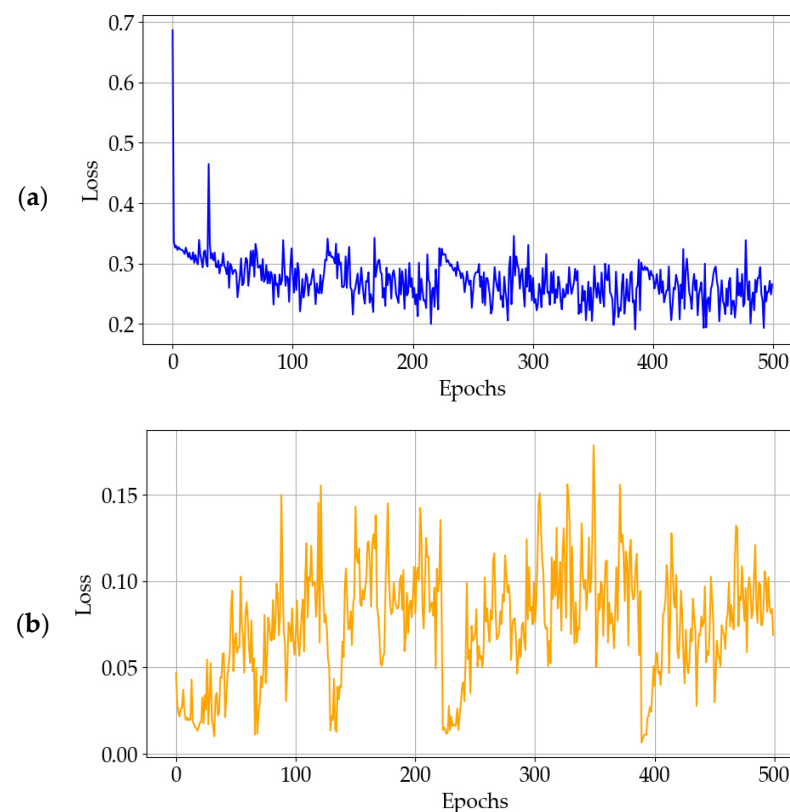


Figure 4. Loss charts of the developed ML model over 500 epochs: (a) training; and (b) validation.

The Validation Loss chart in Figure 4 shows fluctuations throughout the 500 epochs, with no clear downward trend. However, despite these fluctuations, the variation in loss remains within a relatively tight range, suggesting that the model's performance on the validation data, while inconsistent, does not deviate significantly. This indicates that the model's ability to generalize may be reasonably stable.

The model's performance was assessed using a test set that was not exposed to the model during training. The results showed a training MSE of 0.1796 and a testing MSE

of 0.0033, with R^2 scores of 0.8416 for the training set and 0.9939 for the test set. These results demonstrate that the model performed well on the training and unseen test data, particularly excelling in generalizing to new load conditions.

Apart from the two cases, the residual values during the training phase for predicting vertical displacement show very high accuracy. During the training phase, the values are predominantly concentrated near 0. In the testing phase, there is also a suitable density within the range of -2 to 2 , and the results indicate the model's good performance in predicting vertical displacement. The residual plots for training and testing for vertical displacement are shown in Figure 5.

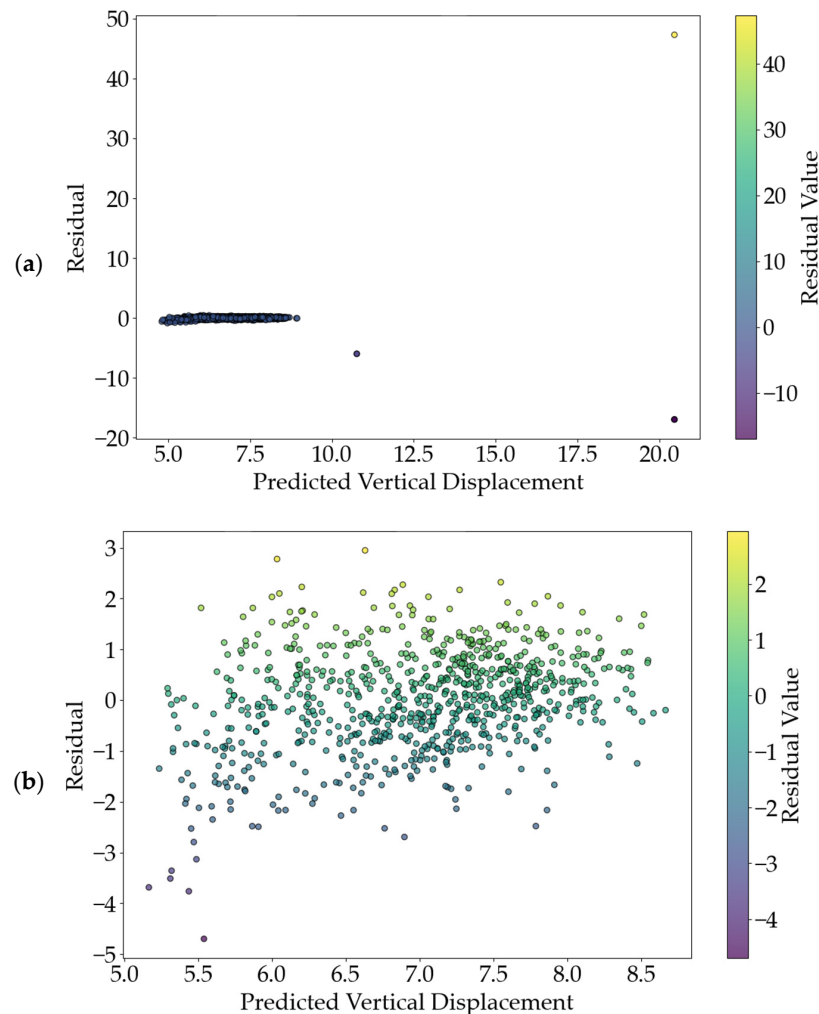


Figure 5. Residual values plotted for (a) training; and (b) test data for vertical displacement.

The residual analysis results for training to predict lateral displacement in the X direction indicate a suitable density within the range of -1 to 1 , while other values are at most within the range of -4 to 3 . This suggests that the model performs well during training for predictions in the X direction. In examining the residuals for the testing phase, a reasonably good density is also observed within the range of -2 to 2 , which ensures the model's adequate performance in predicting structural displacement values in the X direction. The residual plots for training and testing in predicting displacement in the X direction are shown in Figure 6.

The residual values for training the model to predict displacement in the Y direction indicate a suitable density within the range of -2 to 2 , especially in the range of -1 to 1 . Other values are within a maximum range of -4 to 3 . The testing plot for predicting displacement in the Y direction shows a uniform density between -2 and 2 , which exhibits

slightly more dispersion compared to the predictions made for the X direction; however, it still demonstrates acceptable performance. The residual plots related to training and testing for predicting displacement in the Y direction are shown in Figure 7.

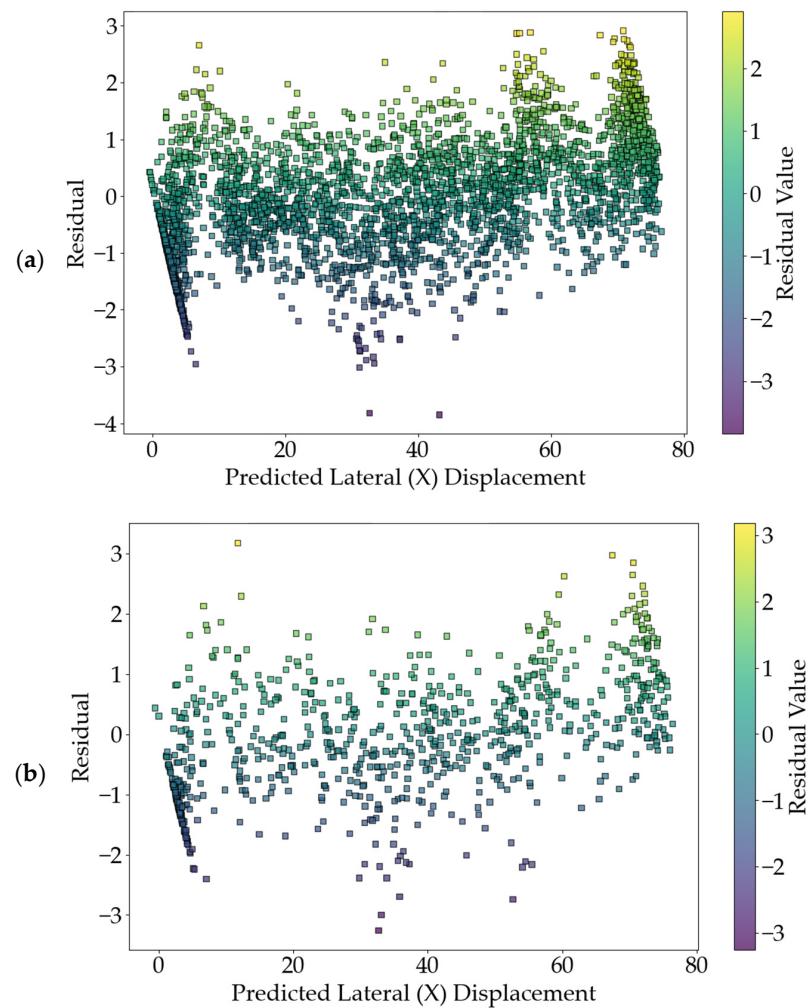


Figure 6. Residual values plotted for (a) training; and (b) test data for lateral (X) displacement.

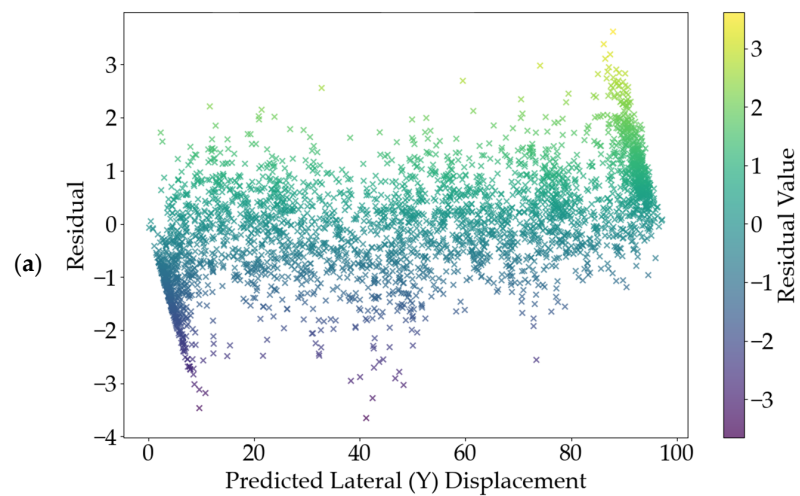


Figure 7. Cont.

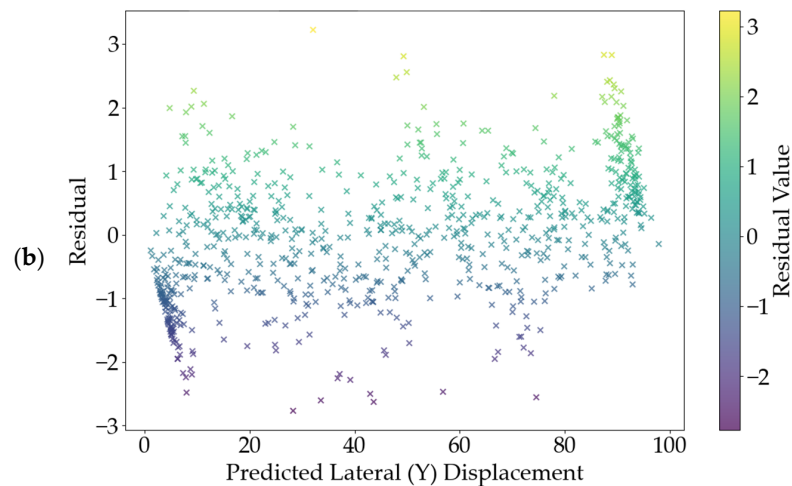


Figure 7. Residual values plotted for (a) training; and (b) test data for lateral (Y) displacement.

In summary, the analysis of the plots indicates that in all three directions, the amount of dispersion is greater at the beginning and end of the charts. This suggests that the developed model has faced challenges in predicting very low or very high displacement values; however, this challenge has not significantly affected the accuracy of the predictions.

3.2. ML Model Evaluation

To evaluate the performance of the developed ML model, 100 test cases were conducted on simulated buildings, predicting displacements in three directions: vertical, lateral (Y), and lateral (X) under various loading scenarios. These predictions were based on a simulated building model, allowing for controlled testing across various structural conditions. The model's accuracy was assessed using the following metrics: Mean Absolute Error (MAE), Root Mean Squared Error (RMSE), coefficient of determination (R^2), and maximum difference from actual value. The obtained values for each of the metrics are presented in Table 4.

Table 4. Developed ML model accuracy assessment metrics.

	MAE	RMSE	R^2	Max Difference
Vertical displacement	0.063	0.081	0.978	0.93%
Lateral (Y) displacement	0.786	0.998	0.999	4.55%
Lateral (X) displacement	0.763	0.900	0.999	7.35%

The model accurately predicted vertical and lateral displacements, achieving an R^2 value of 0.978 for vertical displacement and 0.999 for both lateral (X and Y) displacements. The low Mean Absolute Error (MAE) and Root Mean Square Error (RMSE) values across all directions confirm the model's strong predictive performance, with slightly less precision in predicting vertical displacements than lateral ones. The developed model could predict vertical displacement with only a 0.93% difference from the actual values. The model also predicted lateral (Y) displacements with a 4.55% difference and lateral (X) displacements with a 7.35% difference from the actual values. Figure 8 presents comparative charts of the actual versus predicted values for vertical, lateral (y), and lateral (x) displacements.

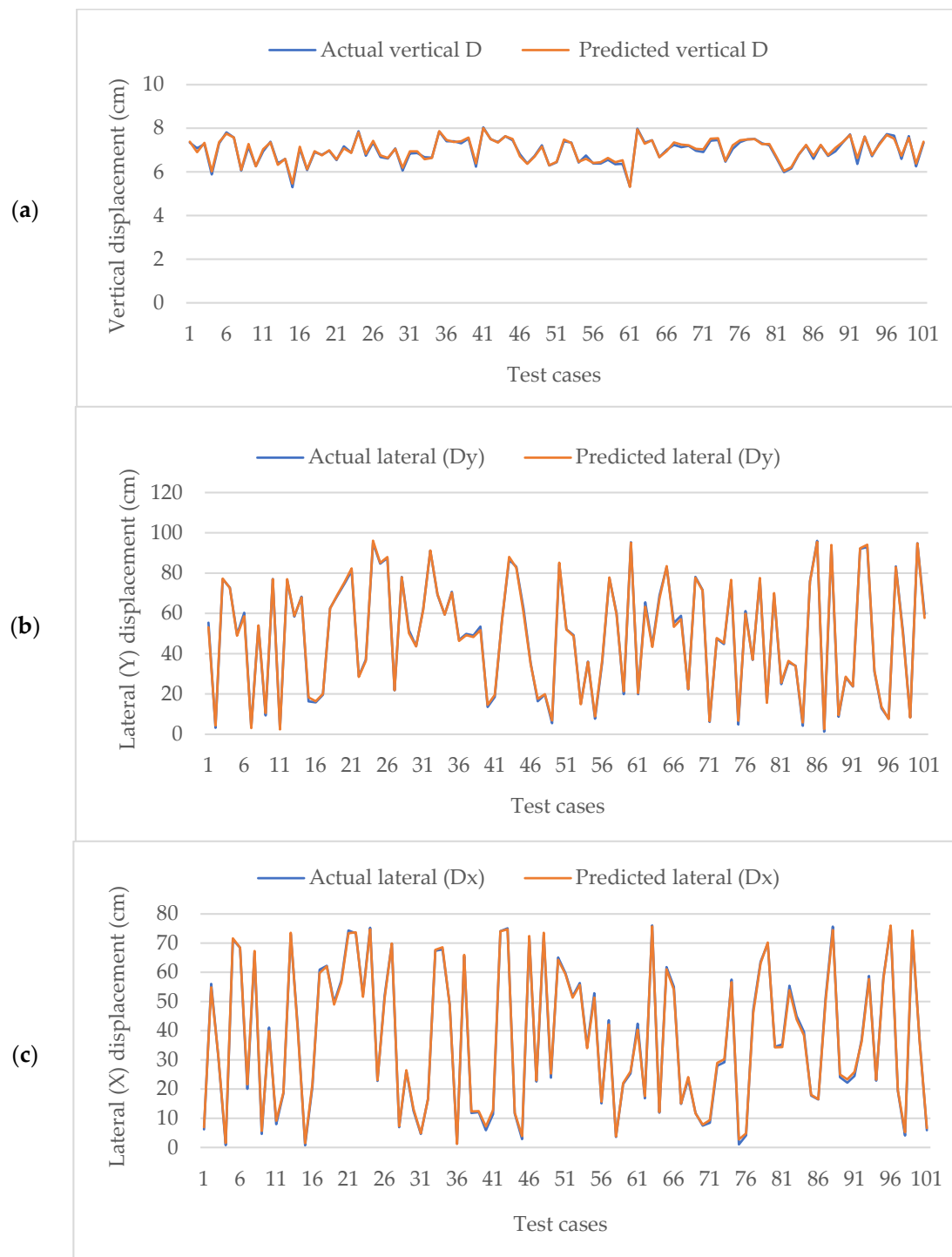


Figure 8. The actual and predicted (a) vertical; (b) lateral (X); and (c) lateral (Y) displacement values.

To further evaluate the performance of the developed predictive model, the amount of lateral displacement in the x and y directions was calculated for all floors and compared with the predicted values in six random test cases, which are shown in Figure 9 for the X direction and Figure 10 for the Y direction. The results show that the developed model has been able to obtain the displacement of the floors with a very small difference compared to the actual values obtained from the finite element analysis.

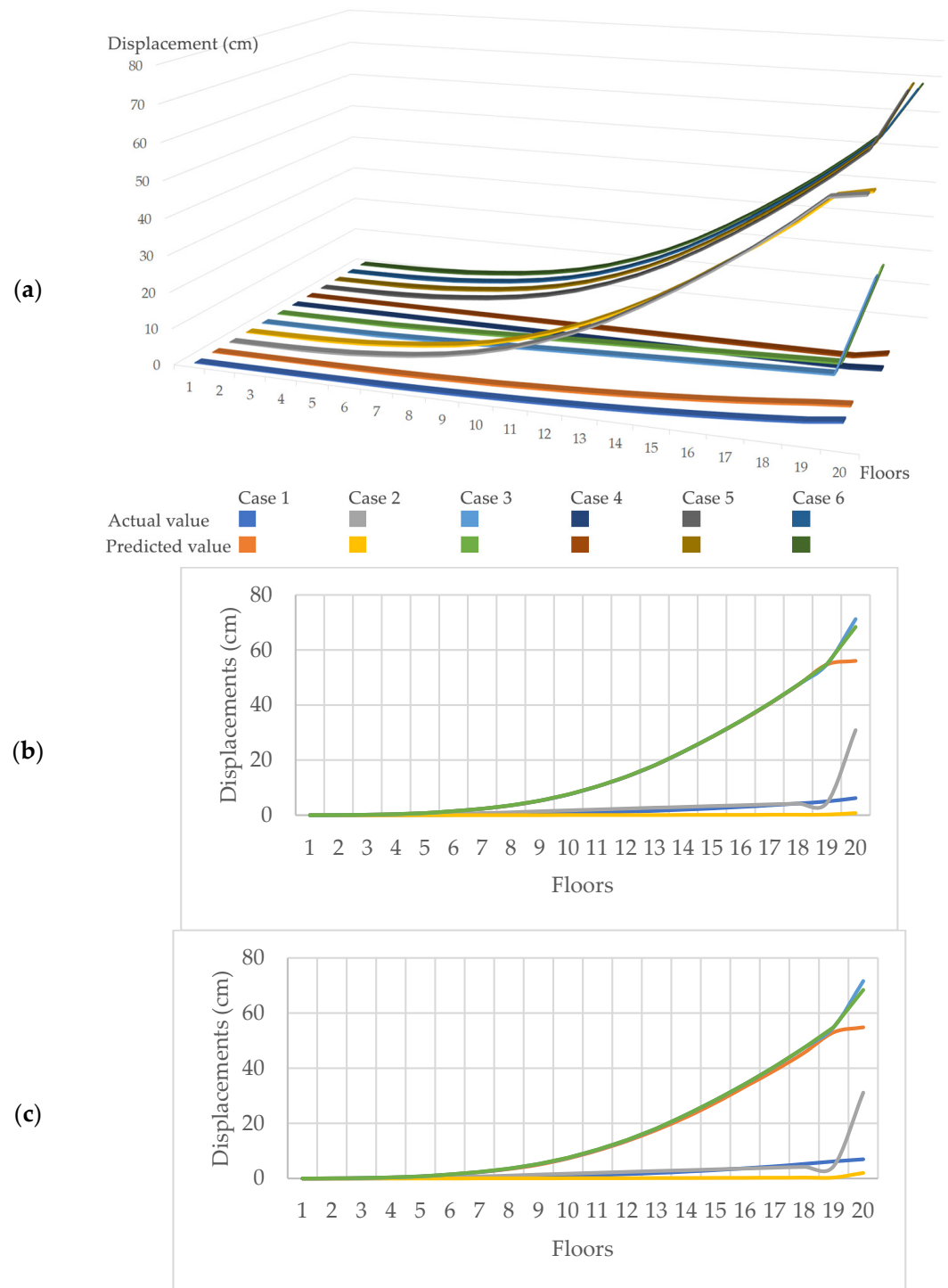


Figure 9. Actual vs. predicted displacement values over the entire structure height in each floor in X direction for six test cases: (a) actual vs. predicted values; (b) actual values; and (c) predicted values. Each colored line in the figures represents a test case.

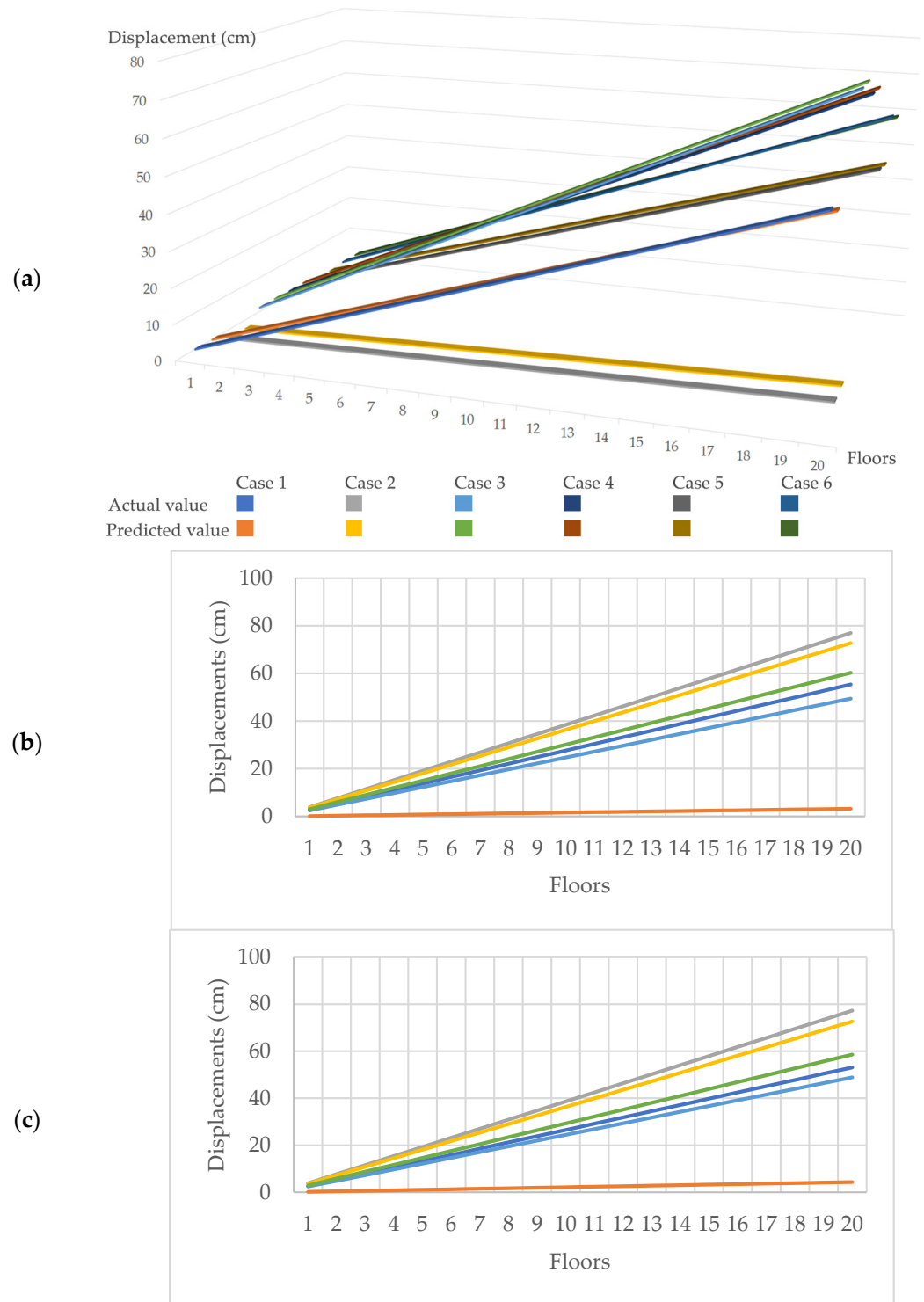


Figure 10. Actual vs. predicted displacement values over the entire structure height in each floor in Y direction for six test cases: (a) actual vs. predicted values; (b) actual values; and (c) predicted values. Each colored line in the figures represents a test case.

3.3. Application of the Model in SHM

The ML model developed in this study is critical to enhancing the monitoring of high-rise building structural health. The buildings’ reactions to different forces could be forecasted without complex simulations each time. This will make continuous tracking of building conditions faster and more efficient, especially in earthquake or strong wind areas. Through this modeling, the actual behavior of the building can be determined with

great accuracy by engineers. This way, it is easier to spot problems early. This model helps maintain the safety of buildings over long periods because it is able to cope with new and unexpected situations. The approach allows engineers to maintain buildings better, reducing the risk of missing structural problems. Integrating this model into monitoring systems would be a reliable and practical way to protect high-rise buildings.

4. Conclusions

In this study, we developed an ML model with an RNN architecture using LSTM layers to estimate the vertical and lateral displacements of high-rise buildings under various loading conditions. To enhance the training of the proposed model, a robust dataset was created by integrating finite element analysis (FEA) with parametric modeling and a multi-objective genetic algorithm (MOGA), ensuring the model's applicability in real-world scenarios. The model was tested on a simulated high-rise building, allowing for detailed analysis across different loading conditions.

The results demonstrated strong model performance. The training Mean Squared Error (MSE) was 0.1796, while the testing MSE was 0.0033. The R^2 scores were 0.8416 for the training set and 0.9939 for the test set, underscoring the model's ability to generalize to unseen data. For vertical displacement prediction, the model achieved a Mean Absolute Error (MAE) of 0.063, a Root Mean Squared Error (RMSE) of 0.081, and an R^2 value of 0.978. In 100 test cases, the model predicted vertical displacement values with only a 0.93% difference from actual values obtained via FEA, demonstrating high accuracy. In predicting lateral (Y) displacements, the model showed a 4.55% difference from actual values. For lateral (X) displacements, the MAE was 0.786, RMSE was 0.998, and R^2 was 0.999, though the model exhibited slightly higher variability, with a 7.35% difference from actual values in 100 test cases. Despite this slight variability, the model's overall low error rates highlight its effectiveness, although further fine-tuning could reduce this variability in future iterations.

The developed model provided reliable predictions of both vertical and lateral displacements, demonstrating a solid capability for generalization to new load conditions. The high R^2 values for all displacement types indicate the model successfully captured the essential relationships between input loads and the corresponding displacement outcomes. However, although the model performed well with low error rates, further refinement is necessary to improve its accuracy in predicting lateral displacements.

This research confirmed the effectiveness of ML for SHM applications, particularly in addressing two critical challenges: data availability and model interpretability. The integration of parametric modeling, FEA analysis, and MOGA ensured the dataset's quality, and the use of LSTM neural networks, known for their ability to handle time series data, allowed for greater interpretability compared to more complex models like DCNN. As sensor technology, FEA methods, and ML algorithms evolve, more sophisticated SHM systems will emerge, ensuring the safety and resilience of high-rise buildings in urban environments.

Several limitations exist in the current model. The structural characteristics of the simulated building were kept constant due to limited computational power, meaning the model cannot currently predict vertical and lateral displacements for other buildings. However, with further development and increased processing power, more variables can be incorporated into the data generation stage, significantly improving the model's generalization to other building types. Expanding the dataset to include a wider variety of building types, geometries, and designs and more diverse loading conditions, such as dynamic forces or seismic events, would enable testing in more challenging scenarios and further enhance the model's applicability. Additionally, incorporating real-time data from high-rise buildings would likely increase prediction accuracy. Future work should also focus on more advanced optimization techniques, hybrid ML models, and different neural network architecture combinations to improve accuracy. This research lays a strong foundation for future studies that explore complex loading conditions and continuously refine predictive models for SHM.

Author Contributions: A.G., Y.S. and M.M.K.: Administration, Conceptualization, Software, Data curation, Validation, Resources, Methodology, Investigation, Writing—original draft. M.F. and S.P.: Administration, Conceptualization, Supervision, Methodology analysis, writing—review, and editing. All authors have read and agreed to the published version of the manuscript.

Funding: This research received no external funding.

Data Availability Statement: Data will be made available on request.

Conflicts of Interest: The authors declare no conflicts of interest.

References

1. Aktan, E.; Bartoli, I.; Glišić, B.; Rainieri, C. Lessons from Bridge Structural Health Monitoring (SHM) and Their Implications for the Development of Cyber-Physical Systems. *Infrastructures* **2024**, *9*, 30. [CrossRef]
2. Liu, Z. Smart Sensors for Structural Health Monitoring and Nondestructive Evaluation. *Sensors* **2024**, *24*, 603. [CrossRef] [PubMed]
3. Zhou, K.; Li, Q.-S. Investigation of Time-Varying Structural Dynamic Properties of High-Rise Buildings under Typhoon Conditions. *J. Build. Eng.* **2022**, *46*, 103796. [CrossRef]
4. Ilgin, H.E.; Ay, B.Ö.; Gunel, M.H. A Study on Main Architectural and Structural Design Considerations of Contemporary Supertall Buildings. *Arch. Sci. Rev.* **2021**, *64*, 212–224. [CrossRef]
5. Halis Gunel, M.; Emre Ilgin, H. A Proposal for the Classification of Structural Systems of Tall Buildings. *Build. Environ.* **2007**, *42*, 2667–2675. [CrossRef]
6. Astorga, A.; Guéguen, P.; Beth, M.; Bessoule, N. Exploring the Effective Implementation of Population-Based SHM in Existing Buildings. *Part II Damage-Feature Classif. Decis.-Making. Eng. Struct.* **2024**, *314*, 118368. [CrossRef]
7. Nicoletti, V.; Arezzo, D.; Carbonari, S.; Gara, F. Dynamic Monitoring of Buildings as a Diagnostic Tool during Construction Phases. *J. Build. Eng.* **2022**, *46*, 103764. [CrossRef]
8. Xu, K.; Li, Q.; Zhou, K.; Han, X. Dynamic Performance of a Supertall Building with an Active Tuned Mass Damper System during Super Typhoon Saola. *Eng. Struct.* **2024**, *318*, 118778. [CrossRef]
9. Zhou, K.; Duan, M.-G.; Wu, Z.-L.; Zhi, L.-H.; Hu, F. Dynamic Behavior Monitoring of Twin Supertall Buildings during Super Typhoon Soksuri Using Social Sensing Data. *J. Build. Eng.* **2024**, *95*, 110119. [CrossRef]
10. Li, Q.S.; Li, X.; He, Y.; Yi, J. Observation of Wind Fields over Different Terrains and Wind Effects on a Super-Tall Building during a Severe Typhoon and Verification of Wind Tunnel Predictions. *J. Wind. Eng. Ind. Aerodyn.* **2017**, *162*, 73–84. [CrossRef]
11. Zhang, C.; Mousavi, A.A.; Masri, S.F.; Gholipour, G.; Yan, K.; Li, X. Vibration Feature Extraction Using Signal Processing Techniques for Structural Health Monitoring: A Review. *Mech. Syst. Signal Process* **2022**, *177*, 109175. [CrossRef]
12. Zhang, C.; Mousavi, A.A.; Masri, S.F.; Gholipour, G. The State-of-the-Art on Time-Frequency Signal Processing Techniques for High-Resolution Representation of Nonlinear Systems in Engineering. *Arch. Comput. Methods Eng.* **2024**, *31*, 1–22. [CrossRef]
13. Mousavi, A.A.; Zhang, C.; Masri, S.F.; Gholipour, G. Damage Detection and Localization of a Steel Truss Bridge Model Subjected to Impact and White Noise Excitations Using Empirical Wavelet Transform Neural Network Approach. *Measurement* **2021**, *185*, 110060. [CrossRef]
14. Ayyildiz, C.; Erdem, H.E.; Dirikgil, T.; Dugenci, O.; Kocak, T.; Altun, F.; Gungor, V.C. Structure Health Monitoring Using Wireless Sensor Networks on Structural Elements. *Ad. Hoc Netw.* **2019**, *82*, 68–76. [CrossRef]
15. Pezeshki, H.; Adeli, H.; Pavlou, D.; Siriwardane, S.C. State of the Art in Structural Health Monitoring of Offshore and Marine Structures. *Proc. Inst. Civ. Eng.-Marit. Eng.* **2023**, *176*, 89–108. [CrossRef]
16. Zapparoli Cunha, B.; Droz, C.; Zine, A.-M.; Foulard, S.; Ichchou, M. A Review of Machine Learning Methods Applied to Structural Dynamics and Vibroacoustic. *Mech. Syst. Signal Process* **2023**, *200*, 110535. [CrossRef]
17. Ruggieri, S.; Bruno, G.; Attolico, A.; Uva, G. Assessing the Dredging Vibrational Effects on Surrounding Structures: The Case of Port Nourishment in Bari. *J. Build. Eng.* **2024**, *96*, 110385. [CrossRef]
18. Wu, X.; Ghaboussi, J.; Garrett, J.H. Use of Neural Networks in Detection of Structural Damage. *Comput. Struct.* **1992**, *42*, 649–659. [CrossRef]
19. Worden, K.; Lane, A.J. Damage Identification Using Support Vector Machines. *Smart Mater. Struct.* **2001**, *10*, 540–547. [CrossRef]
20. Wan, F.L.K. Genetic Algorithms, Their Applications and Models in Nonlinear Systems Identification. 1991. Available online: <https://open.library.ubc.ca/collections/831/items/1.0098602> (accessed on 25 August 2024).
21. Lin, P.; Ding, F.; Hu, G.; Li, C.; Xiao, Y.; Tse, K.T.; Kwok, K.C.S.; Kareem, A. Machine Learning-Enabled Estimation of Crosswind Load Effect on Tall Buildings. *J. Wind. Eng. Ind. Aerodyn.* **2022**, *220*, 104860. [CrossRef]
22. Shahbazi, Y.; Ghofrani, M.; Pedrammehr, S. Aesthetic Assessment of Free-Form Space Structures Using Machine Learning Based on the Expert's Experiences. *Buildings* **2023**, *13*, 2508. [CrossRef]
23. Safaei, M.; Hejazian, M.; Pedrammehr, S.; Pakzad, S.; Etefagh, M.M.; Fotouhi, M. Damage Detection of Gantry Crane with a Moving Mass Using Artificial Neural Network. *Buildings* **2024**, *14*, 458. [CrossRef]
24. Shahbazi, Y.; Abdkarimi, M.; Ahmadnejad, F.; Mokhtari Kashavar, M.; Fotouhi, M.; Pedrammehr, S. Comparative Study of Optimal Flat Double-Layer Space Structures with Diverse Geometries through Genetic Algorithm. *Buildings* **2024**, *14*, 2816. [CrossRef]

25. Zhou, Q.; Li, Q.-S.; Lu, B. Displacement Estimation for a High-Rise Building during Super Typhoon Mangkhut Based on Field Measurements and Machine Learning. *Eng. Struct.* **2024**, *307*, 117947. [[CrossRef](#)]
26. Parisi, F.; Mangini, A.M.; Fanti, M.P.; Adam, J.M. Automated Location of Steel Truss Bridge Damage Using Machine Learning and Raw Strain Sensor Data. *Autom. Constr.* **2022**, *138*, 104249. [[CrossRef](#)]
27. Cabboi, A.; Gentile, C.; Saisi, A. From Continuous Vibration Monitoring to FEM-Based Damage Assessment: Application on a Stone-Masonry Tower. *Constr. Build. Mater.* **2017**, *156*, 252–265. [[CrossRef](#)]
28. Ierimonti, L.; Venanzi, I.; Cavalagli, N.; Comodini, F.; Ubertini, F. An Innovative Continuous Bayesian Model Updating Method for Base-Isolated RC Buildings Using Vibration Monitoring Data. *Mech. Syst. Signal Process* **2020**, *139*, 106600. [[CrossRef](#)]
29. García-Macías, E.; Ubertini, F. Real-Time Bayesian Damage Identification Enabled by Sparse PCE-Kriging Meta-Modelling for Continuous SHM of Large-Scale Civil Engineering Structures. *J. Build. Eng.* **2022**, *59*, 105004. [[CrossRef](#)]
30. Sapidis, G.M.; Kansizoglou, I.; Naoum, M.C.; Papadopoulos, N.A.; Chalioris, C.E. A Deep Learning Approach for Autonomous Compression Damage Identification in Fiber-Reinforced Concrete Using Piezoelectric Lead Zirconate Titanate Transducers. *Sensors* **2024**, *24*, 386. [[CrossRef](#)]
31. Mostafavi, A.; Cha, Y.-J. Deep Learning-Based Active Noise Control on Construction Sites. *Autom. Constr.* **2023**, *151*, 104885. [[CrossRef](#)]
32. Sen, D.; Long, J.; Sun, H.; Campman, X.; Buyukozturk, O. Multi-Component Deconvolution Interferometry for Data-Driven Prediction of Seismic Structural Response. *Eng. Struct.* **2021**, *241*, 112405. [[CrossRef](#)]
33. Yang, J.; Wang, W.; Lin, G.; Li, Q.; Sun, Y.; Sun, Y. Infrared Thermal Imaging-Based Crack Detection Using Deep Learning. *IEEE Access* **2019**, *7*, 182060–182077. [[CrossRef](#)]
34. Yu, Y.; Wang, C.; Gu, X.; Li, J. A Novel Deep Learning-Based Method for Damage Identification of Smart Building Structures. *Struct. Health Monit.* **2019**, *18*, 143–163. [[CrossRef](#)]
35. Mishra, M.; Lourenço, P.B.; Ramana, G.V. Structural Health Monitoring of Civil Engineering Structures by Using the Internet of Things: A Review. *J. Build. Eng.* **2022**, *48*, 103954. [[CrossRef](#)]
36. Giordano, P.F.; Quqa, S.; Limongelli, M.P. The Value of Monitoring a Structural Health Monitoring System. *Struct. Saf.* **2023**, *100*, 102280. [[CrossRef](#)]
37. Thai, H.-T. Machine Learning for Structural Engineering: A State-of-the-Art Review. *Structures* **2022**, *38*, 448–491. [[CrossRef](#)]
38. Robert McNeel & Associates. Grasshopper3d. Available online: <http://www.grasshopper3d.com> (accessed on 22 October 2022).
39. Ministry of Roads & Urban Development of Iran. *Iranian Seismic Code (Standard No. 2800)*, 4th ed.; Ministry of Roads & Urban Development of Iran: Tehran, Iran, 2014.
40. International Code Council (ICC). International Building Code (IBC). Available online: <https://codes.iccsafe.org/content/IBC2021P2> (accessed on 25 August 2024).
41. American Society of Civil Engineers. *Minimum Design Loads and Associated Criteria for Buildings and Other Structures*; American Society of Civil Engineers: Reston, VA, USA, 2017. [[CrossRef](#)]
42. Clemens Preisinger. Karamba3D. Available online: <https://karamba3d.com/> (accessed on 25 August 2024).
43. Chai, T.; Draxler, R.R. Root Mean Square Error (RMSE) or Mean Absolute Error (MAE)?—Arguments against Avoiding RMSE in the Literature. *Geosci. Model. Dev.* **2014**, *7*, 1247–1250. [[CrossRef](#)]
44. Nagelkerke, N.J.D. A Note on a General Definition of the Coefficient of Determination. *Biometrika* **1991**, *78*, 691–692. [[CrossRef](#)]
45. Willmott, C.; Matsuura, K. Advantages of the Mean Absolute Error (MAE) over the Root Mean Square Error (RMSE) in Assessing Average Model Performance. *Clim. Res.* **2005**, *30*, 79–82. [[CrossRef](#)]

Disclaimer/Publisher’s Note: The statements, opinions and data contained in all publications are solely those of the individual author(s) and contributor(s) and not of MDPI and/or the editor(s). MDPI and/or the editor(s) disclaim responsibility for any injury to people or property resulting from any ideas, methods, instructions or products referred to in the content.